Reactions of N(2^2D) with CH_3OH and Its Isotopomers

Hironobu Umemoto,* Koichi Kongo, Shigenobu Inaba, and Yasuyuki Sonoda

Department of Chemical Materials Science, Japan Advanced Institute of Science and Technology, Asahidai, Tatsunokuchi, Nomi, Ishikawa 923-1292, Japan

Toshiyuki Takayanagi and Yuzuru Kurosaki

Advanced Science Research Center, Japan Atomic Energy Research Institute, Tokai, Naka, Ibaraki 319-1195, Japan

Received: April 6, 1999; In Final Form: June 17, 1999

The reaction pathways of N(^{2}D) with methanol and its isotopomers were specified by laser pump-and-probe experiments and molecular orbital calculations. It was shown experimentally that CH_3OH deactivates N(^{2}D) efficiently to produce ground-state NH and OH radicals. The nascent state distributions of these radicals are not statistical, suggesting that the intermediate species decompose before energy randomization. A similar result was obtained for ND and OD formed in the N(^{2}D)/CD_3OD system. NH, ND, OH, and OD radicals were identified in partially deuterated systems. The ND/NH population ratio measurements show that NH and ND radicals are produced from both hydroxyl and methyl positions, but the former plays more important roles, one order of magnitude, than the latter. This is consistent with the result of ab initio molecular orbital calculations that the most favorable initial step is the addition of N(^{2}D) to the O atom. The OD/OH ratio in the CD_3OH system as well as the OH/OD ratio in the CH_3OD system is 0.5. OH(OD) is produced mainly by the C−O bond scission just after the insertion of N(^{2}D) into a C−H(C−D) bond, but the bond scission after intramolecular H/D scrambling is also important. This is also consistent with the result of calculations that the barrier height for the H(D) atom migration is much lower than the available energy.

Introduction

Recently, we have studied the reactions of metastable atomic nitrogen, N(^{2}D), with simple polyatomic hydride molecules, both experimentally[1−7] and theoretically.[6−11] It was revealed experimentally that the production of ground-state NH radicals is one of the main exit channels in the reactions with methane and water[1−4]

$$N(^2D) + CH_4 \rightarrow NH(X\,^3\Sigma^-) + CH_3$$

$$N(^2D) + H_2O \rightarrow NH(X\,^3\Sigma^-) + OH(X\,^2\Pi)$$

In addition, production of H atoms could also be identified

$$N(^2D) + CH_4 \rightarrow H + CH_2{=}NH$$

$$N(^2D) + H_2O \rightarrow H + HNO$$

The nascent internal and translational energy distributions of the reaction products were measured, together with the quantum yields. The experimental results as well as those of ab initio molecular orbital calculations suggest that insertion of N(^{2}D) into a C−H bond is important for the reactions with alkane hydrocarbons, while addition to the O atom is the primary step for water.[2−4,8,10]

Since methanol has both C−H and O−H bonds, i.e., bifunctional, it is interesting to examine which bond plays more important roles in the deactivation of N(^{2}D). The production of H in the reaction with CH_4 can be related to the triradical character of atomic nitrogen.[3] One unpaired electron remains after the insertion of N(^{2}D) into a C−H bond. This electron interacts with the electron of the carbon atom to form a C═N double bond. The prompt ejection of an H atom follows. If a similar process can be assumed for CH_3OH, OH is expected to be produced. Of course, NH shall also be produced after the insertion of N(^{2}D) into a C−H bond. In the reaction with H_2O, the main exit is the production of NH and OH.[4] After the addition of N(^{2}D) to the O atom, one of the H atoms migrates to produce an HNOH complex, which decomposes to NH+OH. A similar process to produce CH_3O + NH should be possible for CH_3OH. These two processes, insertion into a C−H bond and addition to the O atom, can be distinguished by using partially deuterated compounds, CD_3OH and CH_3OD.

In the reaction of O(^{1}D$_2$) with methanol, OH radicals are produced efficiently.[12] By using isotopically substituted methanols, Goldstein and Wiesenfeld showed that 70% of OH(OD) originates from the hydroxyl position, reaction 1 or 2, while 30% originates from the methyl positions, reaction 3.[12] They have also concluded that abstractive processes are minor based on the low vibrational excitation of OH(OD).

$$O(^1D_2) + CH_3OH \rightarrow CH_3O + OH \quad (1)$$

$$\rightarrow HOCH_2 + OH \quad (2)$$

$$\rightarrow HO + CH_2OH \quad (3)$$

Matsumi et al. have demonstrated that ejection of H atoms takes place when C−H bonds are attacked, reactions 4 and 5, although the absolute yield is not large, 0.18.[13]

* Corresponding author. E-mail: umemoto@jaist.ac.jp.

10.1021/jp991156s CCC: $18.00
Published on Web 08/10/1999

$$O(^1D_2) + CH_3OH \rightarrow HOCHOH + H \quad (4)$$

$$\rightarrow HOCH_2O + H \quad (5)$$

A clear isotope effect has been observed in the reaction rates of N(^{2}D) with methane isotopomers.[3,5,7] C−H bonds are 1.7 ± 0.1 times more reactive than C−D bonds against N(^{2}D). It has also been shown that H_2O is 1.4 times more reactive than D_2O.[5] On the other hand, no clear H/D isotope effect was observed in the reactions of O($^1D_2$) with partially deuterated methanols.[12] It is interesting to examine such an isotope effect in addition to the difference in the reactivity between C−H and O−H bonds.

In the present work, reactions of N(^{2}D) with CH_3OH and its isotopomers (CH_3OD, CD_3OH, and CD_3OD) were studied both from experimental and theoretical sides. The nascent internal state distributions of NH($X\ ^3\Sigma^-$), ND($X\ ^3\Sigma^-$), OH($X\ ^2\Pi$), and OD($X\ ^2\Pi$) were determined. The ND/NH and OD/OH population ratios were measured in partially deuterated systems. The rate constants for the overall deactivation were also measured. Ab initio molecular orbital calculations were carried out to predict the geometries and the potential energies of the stationary points and the transition states on the reaction paths.

Experimental Section

The experimental apparatus and the procedure were similar to those described elsewhere.[1−5,14−16] NO was two-photon photolyzed with the frequency doubled output of a dye laser (Quanta-Ray, PDL-3/GCR-170) at 275.3 nm. NH(ND) and OH(OD) radicals were detected by laser-induced fluorescence. A dye laser (Lambda Physik, LPD3000E) pumped with a XeF excimer laser (Lambda Physik, LPX105i) or a Nd:YAG laser (Quanta-Ray, GCR-170) was used to probe these radicals. The output of this laser was doubled in frequency by a KDP crystal. The wavelength was tuned to the A $^3\Pi_i$−X $^3\Sigma^-$ transition around 336 nm for NH(ND) and to the A $^2\Sigma^+$ −X $^2\Pi$ transition around 308 nm for OH(OD).

In the measurements of the rotational state distributions of NH(ND), the interpulse delay was fixed at 150 ns, while the total pressure was kept at 53 Pa. When OH(OD) was detected, the delay time was 300 ns while the pressure was 27 Pa. Under such conditions, secondary relaxation processes can be ignored. In the measurements of the vibrational state distributions, these radicals were rotationally relaxed by adding 2.6 kPa of He. The delay time between the two laser pulses was 1 μs. The population ratios were determined by comparing the experimentally obtained LIF spectra to the simulated ones. The ND/NH and OD/OH population ratios were typically measured under rotationally relaxed conditions. Some measurements were also performed under single collision conditions.

The decay rates of N(^{2}D) concentration were measured to evaluate the overall rate constant. The procedure was the same as that described elsewhere.[5] NO pressure was kept constant at 27 Pa, while 27 kPa of Ar was added to reduce the diffusional loss of N(^{2}D). The methanol pressure was changed between 0 and 133 Pa.

NO (Sumitomo Seika, 99.999%), He (Teisan, 99.995%), and Ar (Teisan, 99.9995%) were used from cylinders without further purification. CH_3OH (Nacalai Tesque, 99.8%), CH_3OD (Euriso-Top, 99%), CD_3OH (Euriso-Top, 99.8%), and CD_3OD (Euriso-Top, 99.8%) were used after fractional distillation. As for CH_3OH, molecular sieve 3A was also used to remove water, but there was no change in the results. Since Pyrex glass is reactive to methanol vapor to exchange OH and OD,[17] Pyrex glass was avoided to use in the gas handling system in the measurements for CH_3OD and CD_3OD.

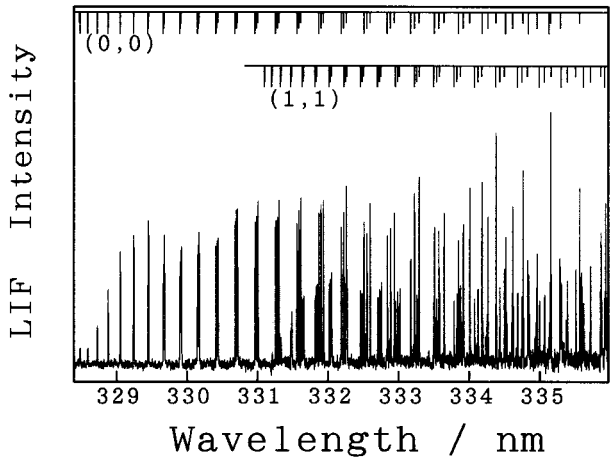

Figure 1. LIF spectrum of NH($X\ ^3\Sigma^-$) formed in the reaction of N(^{2}D) + CH_3OH. The pressures were 22 Pa for NO and 31 Pa for CH_3OH. The photolysis probe delay time was 150 ns. The assignments are shown for the R_1, R_2, and R_3 branches of the (0,0) and (1,1) bands.

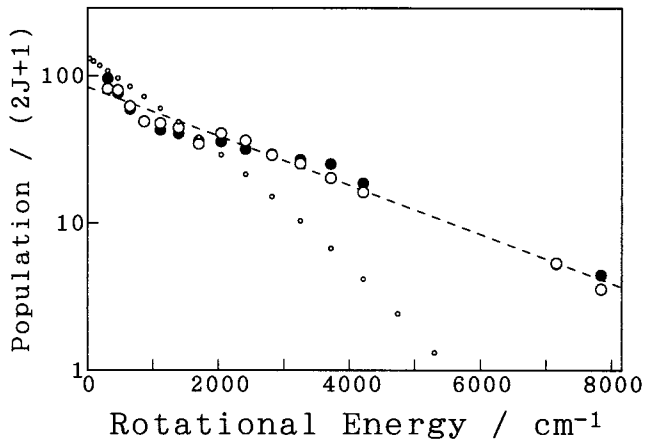

Figure 2. Boltzmann plots of relative populations of NH($X\ ^3\Sigma^-$, v''=0) formed in the reactions of N(^{2}D) with CH_3OH(●) and CD_3OH(○). Small circles represent the prior distribution for the N(^{2}D) + $CH_3OH \rightarrow NH + CH_3O$ process. The broken line represents the rotational temperature of 3700 K.

Experimental Results

NH and OH radicals were identified in the N(^{2}D)/CH_3OH system. In the CD_3OD system, ND and OD were identified. All of the radicals, NH, ND, OH, and OD, were detected in the CD_3OH and CH_3OD systems.

Figure 1 shows a typical LIF spectrum of NH($X\ ^3\Sigma^-$) measured in the presence of 22 Pa of NO and 31 Pa of CH_3OH. The fluctuation in the probe laser intensity is corrected in this figure. The spectral assignments for the R_1, R_2, and R_3 branches of the (0,0) and (1,1) bands, given by Brazier et al., are shown in the figure.[18] The nascent state distributions can be evaluated from the peak heights of such spectra.[1,15] Figure 2 shows the Boltzmann plots of relative populations of NH($X\ ^3\Sigma^-$, $v'' = 0$) formed in the reactions with CH_3OH and CD_3OH. There is no practical difference between the results of CH_3OH and CD_3OH, suggesting that O−H bonds play more important roles in the production of NH than C−H bonds. The broken line represents the rotational temperature of 3700 K. In general, the nascent distribution may not be Boltzmann-like, but, in the present case, that can be approximated by a

TABLE 1: Population Ratios of NH, ND, OH, and OD

	NH(v=1)/NH(v=0)	ND(v=1)/ND(v=0)	OH(v=1)/OH(v=0)	OD(v=1)/OD(v=0)	ND/NH	OD/OH
CH_3OH	0.4 ± 0.1		0.15 ± 0.05			
CD_3OH	0.4 ± 0.1				0.10 ± 0.03	0.5 ± 0.1
CH_3OD		0.4 ± 0.1			3.0 ± 0.8	2.0 ± 0.5
CD_3OD		0.4 ± 0.1		0.15 ± 0.05		

Boltzmann distribution at 3700 K. The prior distribution for the $N(^2D) + CH_3OH \rightarrow NH + CH_3O$ process is also illustrated in Figure 2. In the calculation of the prior distribution, the available energy was assumed to be partitioned into all the degrees of freedom evenly. The calculation procedure was similar to that employed by Bogan and Setser.[19] The vibrational frequencies of CH_3O employed were 825, 978, 1142, 1403, 1418, 1532, 3020, 3109, and 3140 cm^{-1} which were obtained by ab initio calculations at the MP2(full)/cc-pVDZ level. The vibrational population ratios, NH(v''=1)/NH(v''=0), were 0.4 ± 0.1 in both systems. This is much larger than the prior one, 0.09. The energy distributions of ND formed in the CH_3OD and CD_3OD systems were similar to those of NH in the CH_3OH and CD_3OH systems. The rotational state distribution of NH(v''=0) formed in the $N(^2D)/CH_3OD$ system was similar to that obtained in alkane systems.[2] The quantitative determination of the state distribution of ND in the $N(^2D)/CD_3OH$ system was difficult because of its low production yield. The measured vibrational population ratios are summarized in Table 1, together with the ND/NH and OD/OH ratios in the CD_3OH and CH_3OD systems.

The ND/NH population ratio in the $N(^2D)/CD_3OH$ system was 0.10 ± 0.03 under rotationally relaxed conditions. Since the number of C−D bonds is three times more than that of O−H, O−H bonds are 30 ± 10 times more efficient than C−D bonds in the production of NH(ND). On the other hand, in the $N(^2D)/CH_3OD$ system, the ND/NH ratio was 3.0 ± 0.8. O−D bonds are just 9 ± 2 times more efficient in producing NH(ND) than C−H bonds. The ND/NH population ratio was independent of the methanol pressure between 30 and 100 Pa, showing that the isotope scrambling reactions, such as NH + $CH_3OD \rightarrow ND + CH_3OH$, are minor. The temporal profiles of the induced fluorescence for NH and ND were indistinguishable, and the correction for the quenching of the upper $A\ ^3\Pi$ state is not necessary.

The LIF signal intensities of NH for CH_3OH and CD_3OH were compared under single collision conditions. The signal intensity for CH_3OH was 20 ± 10% larger than that for CD_3OH. This result again suggests that C−H bonds have minor contribution to the production of NH. In this measurement, it is not necessary to take into account the difference in the rotational state distributions or that in the deactivation rate constants, since the differences are minor.

The Boltzmann plot of the relative population of OH(v''=0) formed in the $N(^2D)/CH_3OH$ system is illustrated in Figure 3. This distribution can be approximated by a superposition of two Boltzmann distributions. The broken line in Figure 3 is the superposition of Boltzmann distributions at 400 and 3000 K. The distribution of the hot component is similar to the prior one. A similar result was obtained in the $N(^2D)/CD_3OD$ system. The nascent rotational state distribution of OD(v''=0) can be represented by a superposition of two components at 400 and 3000 K. Production of vibrationally excited OH(OD) was minor; the v''=1/v''=0 population ratios were 0.15 ± 0.05.

Not only OH but also OD could be observed in the $N(^2D)/CD_3OH$ system. The OD/OH ratio was measured to be 0.5 ± 0.1. OD radicals observed are not the reaction product of $O(^1D_2)$ with CD_3OH. $O(^1D_2)$ is produced in the two-photon dissociation

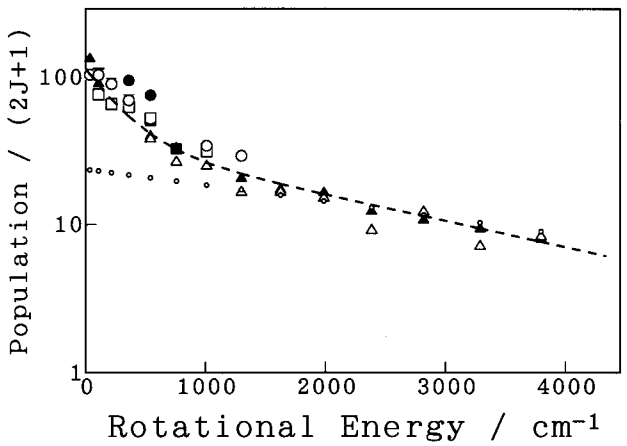

Figure 3. Boltzmann plot of relative population of OH($X\ ^2\Pi$, v''=0) formed in the reaction of $N(^2D)$ with CH_3OH: P_1 (■); Q_1 (▲); R_1 (●); P_2 (□); Q_2 (△); R_2 (○). Small circles represent the prior distribution for the $N(^2D) + CH_3OH \rightarrow CH_2{=}NH + OH$ process. The broken line represents the superposition of two Boltzmann distributions, $(2J + 1)\{3\exp(-E_N/400R) + \exp(-E_N/3000R)\}$, where E_N is the rotational energy and R is the gas constant.

TABLE 2: Rate Constants for the Deactivation of $N(^2D)$ at Room Temperature

	rate constant/10^{-12} $cm^3\ s^{-1}$
CH_3OH	91.7 ± 4.6
CD_3OH	99.4 ± 5.0
CH_3OD	74.3 ± 5.8
CD_3OD	78.4 ± 3.0
CH_4[a]	3.33 ± 0.22
CD4[a]	1.97 ± 0.28
H_2O[a]	41.7 ± 1.2
D_2O[a]	29.3 ± 0.8

[a] Reference 5.

of NO, but the production efficiency is small; around 0.5% of $N(^2D)$.[3] To check the possibility of the $O(^1D_2) + CD_3OH$ reaction, the OD/OH ratio was measured in the $N(^2D)/CH_3OH/D_2$ system. The OD signal was negligibly small compared to that of OH. The rate constant for the $O(^1D_2) + D_2$ reaction is 9.4×10^{-11} $cm^3\ s^{-1}$ which is almost the same as that for $N(^2D) + CH_3OH$, 9.2×10^{-11} $cm^3\ s^{-1}$.[20] Production of OH(OD) in the NH(ND) + NO $\rightarrow N_2$ + OH(OD) reaction can also be ruled out by the above observation. In any case, the yield of OH(OD) in the NH(ND) + NO reaction is small.[21−23] A similar result was obtained for CH_3OD. The OH/OD ratio was 0.5 ± 0.1.

The rate constants for the overall deactivation of $N(^2D)$ were determined under pseudo-first-order conditions. The results are summarized in Table 2. The error limit is one standard deviation. The results for CH_4, CD_4, H_2O, and D_2O are also listed for comparison.[5] The rate constants for CH_3OH and CD_3OH are similar and larger than those for CH_3OD and CD_3OD. This result is consistent with the model that O−H(O−D) bonds are more important than C−H(C−D) bonds in the deactivation of $N(^2D)$. A similar tendency has been observed in the quenching of Cd($5\ ^3P_J$) by methanol isotopomers.[24]

The detection of atomic hydrogen produced in the present systems was unsuccessful because atomic hydrogen is produced

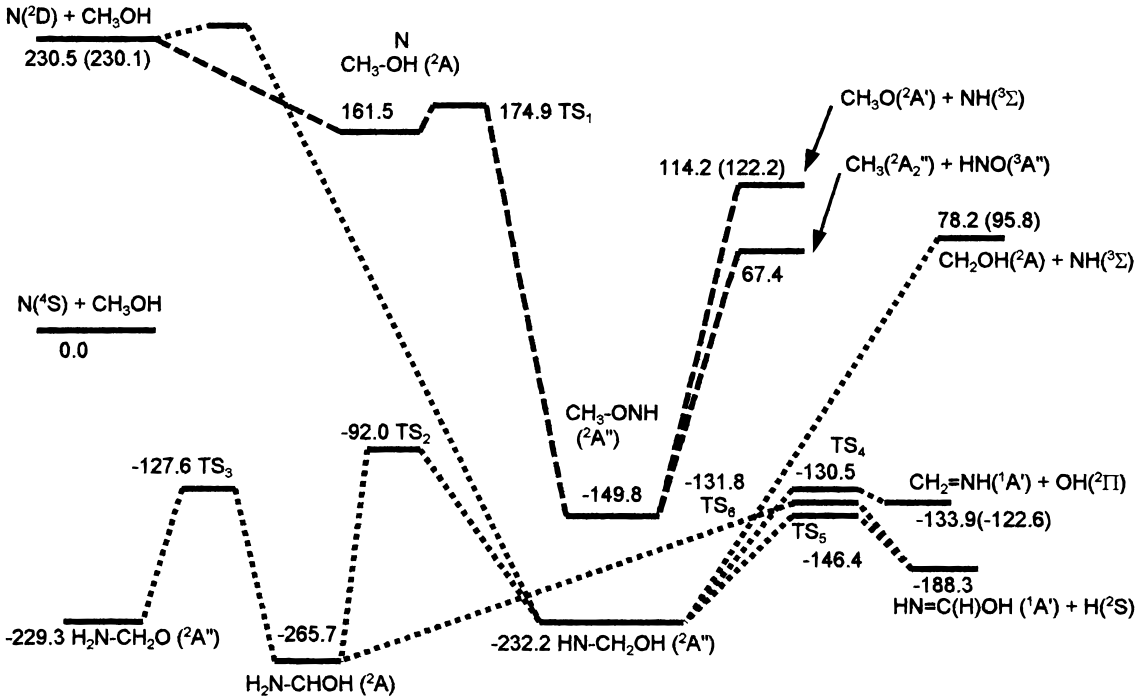

Figure 4. Schematic energy diagram (in kJ mol^{-1}) for the N(^{2}D) + CH_3OH reaction at the PMP4(full, SDTQ)/cc-pVTZ//MP2(full)/cc-pVDZ level of theory. The energy of the N(^{4}S) + CH_3OH asymptote is defined to be zero. Values in parentheses are experimental ones.

by direct two-photon photolysis of methanol. The production of HNO could not be identified, either. The sensitivity to detect this species by LIF must be much lower than that for NH and OH.

Calculations

The potential energies were calculated under various geometries to obtain information on the reaction pathways. The computational method is similar to that used previously.[6−10] The Møller−Plesset perturbation method was used to calculate the reaction energy diagram and thus to understand possible product channels. All electrons were included in all of the MP calculations to avoid errors resulting from frozen core approximation. The geometries of the reactants, products, intermediates, and transition states have been fully optimized at second-order Møller−Plesset (MP2(full)) level of theory with the correlation-consistent polarized valence double-ζ (cc-pVDZ) basis set.[25] Single point calculations for the MP2(full)/cc-pVDZ geometries were also carried out using the spin-projected fourth-order MP method including single, double, triple, and quadruple substitutions (PMP4(full,SDTQ)[26]) with the correlation-consistent polarized valence triple-ζ (cc-pVTZ) basis set[25] in order to obtain more accurate energy values. All ab initio calculations were performed using the *Gaussian 94* program package.[27]

Figure 4 shows the schematic energy diagram for the lowest doublet potential energy surface of the N(^{2}D) + CH_3OH reaction. The MP2(full)/cc-pVDZ optimized geometries of transition states are shown in Figure 5. The total electronic energies of all the species shown in Figure 4 are summarized in Table 3. $< \mathbf{S^2} >$ is the expected value of the spin operator which should be 0.75 for pure doublet states and 3.75 for pure quartet states. It was difficult to find the transition state for the insertion of N(^{2}D) into a C−H bond. However, from analogy with the CH_4 system, there must be a small barrier for insertion.[7,8] This barrier is included in Figure 4. Figure 4 also includes energies obtained from experimental thermochemical data,[28] although the available experimental data are limited. The relative energies of the present ab initio calculations are reliable within 18 kJ mol^{-1}.

Discussion

The following processes are important in the present N(^{2}D)/CH_3OH system:

$$N(^2D) + CH_3OH \rightarrow CH_3O + NH + 116 \text{ kJ mol}^{-1} \quad (6)$$

$$\rightarrow CH_3 + HNO + 163 \text{ kJ mol}^{-1} \quad (7)$$

$$\rightarrow NH + CH_2OH + 152 \text{ kJ mol}^{-1} \quad (8)$$

$$\rightarrow CH_2{=}NH + OH + 364 \text{ kJ mol}^{-1} \quad (9)$$

$$\rightarrow HN{=}C(H)OH + H + 419 \text{ kJ mol}^{-1} \quad (10)$$

In reactions 6 and 7, the hydroxyl position is attacked, while in reactions 8, 9, and 10, the methyl position is attacked.

From analogy with the CH_4 and H_2O systems, the initial step for reactions 6 and 7 should be the addition of N(^{2}D) to the O atom, while that for reactions 8, 9, and 10 should be the insertion into a C−H bond. Ab initio molecular orbital calculations support the above predictions. The most attractive process is the addition of N(^{2}D) to the O atom. N(^{2}D) may interact with the unshared electron pair on the O atom to form an addition complex. H atom migration takes place without a high energy barrier to produce an insertive CH_3ONH complex. Two major exit channels must be CH_3O + NH and CH_3 + HNO. Of course, reactions 8, 9, and 10, initiated by the interaction of N(^{2}D) with C−H bonds, cannot be ignored.

The nascent rotational state distribution of NH(v''=0) is hotter than that observed in the N(^{2}D)/H_2O system.[4] This should be related to the larger exothermicity in the present reaction. The exothermicity for the N(^{2}D) + $H_2O \rightarrow$ NH + OH reaction is only 61 kJ mol^{-1}. There are at least two components in the

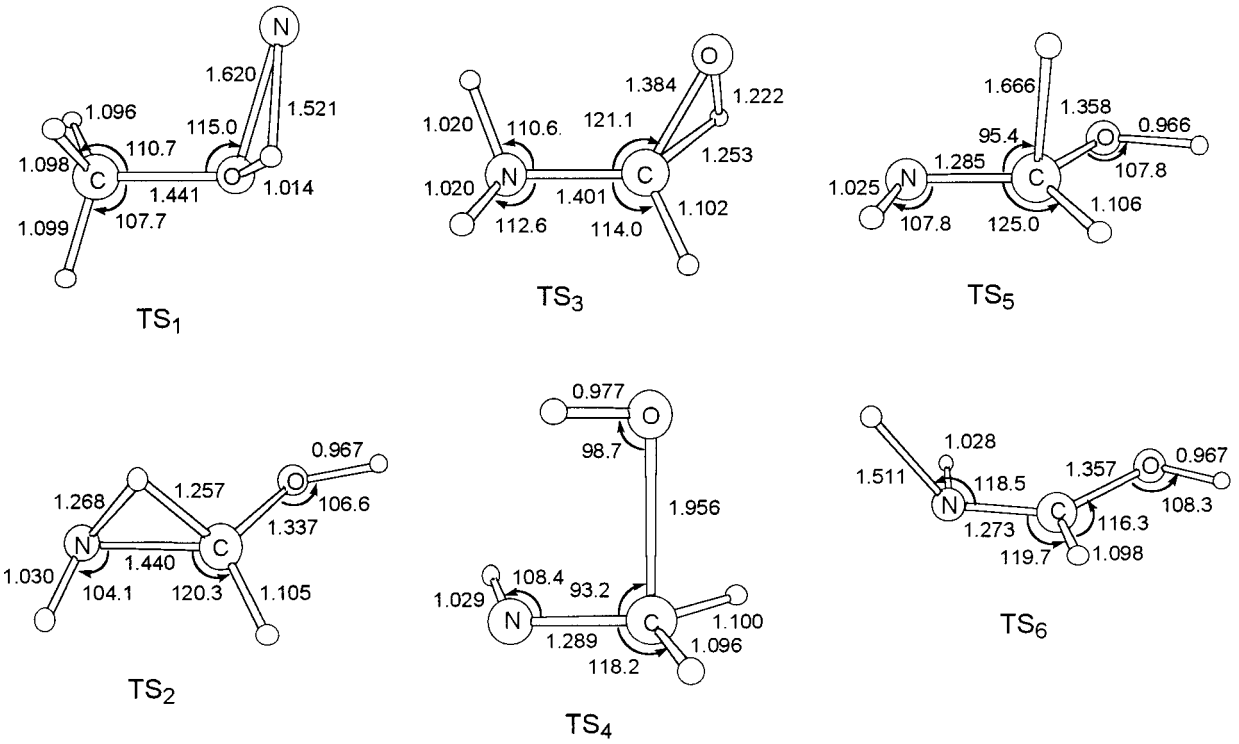

Figure 5. Molecular geometries of the transition states on the lowest doublet potential energy surface for N + CH_3OH optimized at the MP2-(full)/cc-pVDZ level of theory.

TABLE 3: Total Energies (atomic unit), Expected Values of the Spin Operator, and the Symmetry for the N + CH_3OH Reaction

molecule	MP2[a]	PMP4[b]	$\langle S^2\rangle$[c]	symmetry
Fragment				
N(^{4}S)		−54.52447	3.756	
N(^{2}D)		−54.43659	1.766	
H(^{2}S)		−0.49981	0.750	
NH($X\,^3\Sigma^-$)	−55.07219	−55.15230	2.016	$C_{\infty v}$
OH($X\,^2\Pi$)	−75.54487	−75.65032	0.756	$C_{\infty v}$
HNO(^{3}A″)	−130.11909	−130.29727	2.035	*Cs*
CH_3 ($^2A_2''$)	−39.69309	−39.77624	0.762	D_{3h}
CH_3O(^{2}A′)	−114.72172	−114.90321	0.759	*Cs*
CH_2OH(^{2}A)	−114.73822	−114.91764	0.761	C_1
CH_2═NH(^{1}A′)	−94.34602	−94.50315	0.000	*Cs*
CH_3OH(^{1}A′)	−115.39292	−115.58139	0.000	*Cs*
HN═C(H)OH(^{1}A′)	−169.41972	−169.67216	0.000	*Cs*
Intermediate				
CH_3O(N)H(^{2}A)	−169.77954	−170.04749	0.759	C_1
CH_3ONH(^{2}A″)	−169.90211	−170.16689	0.763	*Cs*
$HNCH_2OH$(^{2}A″)	−169.93211	−170.19744	0.762	*Cs*
H_2NCHOH(^{2}A)	−169.94865	−170.21138	0.760	C_1
H_2NCH_2O(^{2}A″)	−169.93254	−170.19727	0.759	*Cs*
Transition State				
TS_1(^{2}A)	−169.77128	−170.03958	0.761	C_1
TS_2(^{2}A)	−169.87166	−170.14070	0.798	C_1
TS_3(^{2}A)	−169.88529	−170.15399	0.788	C_1
TS_4(^{2}A)	−169.87902	−170.15289	0.926	C_1
TS_5(^{2}A)	−169.87581	−170.15724	0.962	C_1
TS_6(^{2}A)	−169.88857	−170.15859	0.904	C_1

[a] cc-pVDZ basis set. [b] cc-pVTZ basis set. [c] Calculated at the HF/cc-pVTZ/MP2/cc-pVDZ level of theory.

rotational distribution of OH(v''=0). One is hotter and one is colder than that observed in the H_2O system.[4] Reaction 9 is also much more exothermic than the N(^{2}D) + H_2O → NH + OH reaction, but is less direct. Production of OH requires the energy flow from the site of insertion. If the C−O bond breaks before intramolecular energy randomization, OH shall not be internally excited. The cold component may be related to the C−O bond breakage just after the insertion of N(^{2}D) into a C−H bond. The distribution of the hot component is rather similar to the prior one, suggesting that the lifetime of the intermediate is long enough for energy randomization. The hot component may be produced after the H atom migration, which will be discussed later.

All of the experimental results, ND/NH population ratios for partially deuterated methanols, resemblance in the rotational state distributions of NH in the CH_3OH and CD_3OH systems, relative NH yields for CH_3OH and CD_3OH, as well as the overall rate constants, suggest that reaction 6 is more dominant than reaction 8. In addition, there must be H/D isotope effects in the production processes of NH(ND). O−H bonds are 30 ± 10 times more efficient than C−D bonds in the production of NH(ND), while O−D bonds are just 9 ± 2 times more efficient than C−H bonds. Such isotope effects may be ascribed to both methyl and hydroxyl parts. Recently, we have reported that the production of H−N−C type complexes is 1.6 times more efficient than that of D−N−C type complexes in the reactions with methane isotopomers.[3] According to the overall rate constant measurements, C−H bonds are 1.7 times more reactive than C−D bonds.[5,7] The rate constant for the deactivation by H_2O is larger than that by D_2O by a factor of 1.4.[5]

The isotope effect observed in the present systems is in contrast to the result in the O($^1D_2$) systems. In the reactions of O($^1D_2$), although O−H and O−D bonds are more reactive than C−H and C−D bonds, no clear H/D isotope effect has been observed.[12] This may partly be attributed to the high reactivity of O($^1D_2$) against both O−H(O−D) and C−H(C−D) bonds. The observed isotope effect in the N(^{2}D) systems must be ascribed to the difference in the zero-point energies or that in vibrational partition functions. At least, in the O($^1D_2$) systems, activation energies are not expected because the rate constants are as large as gas kinetic ones.[13,29] The difference in vibrational frequencies must cancel between the reactant and the transition state.

Production of OH in the CH_3OH and CD_3OH systems can easily be explained if the C−O bond breaks after the insertion of N(^{2}D) into a C−H(C−D) bond. Since a C═N double bond is formed, this channel is more exothermic than the NH(ND) production channels. It is more puzzling to explain the production of OD in the CD_3OH system. The only possible explanation includes H(D) atom migration after the insertion of N(^{2}D)

$$N(^2D) + CD_3OH \rightarrow D\dot{N}-CD_2-OH \rightarrow D_2N-\dot{C}D-OH$$
$$\rightarrow D_2N-CHD-\dot{O} \rightarrow D_2N-\dot{C}H-OD$$
$$\rightarrow D\dot{N}-CHD-OD \rightarrow DN{=}CHD + \dot{O}D$$

Production of OD is statistically more expected than that of OH. The situation must be similar in the CH_3OD system. Not only OD but also OH shall be produced if H(D) atom migration is rapid. As Figure 4 shows, the energies of the transition states for these H(D) atom migration processes are all much lower than the available energy. These migration processes can be related to the triradical character of atomic nitrogen. Such migration cannot be expected in the reactions of O(^{1}D$_2$).

The OD/OH population ratio in the CD_3OH system agrees with the OH/OD ratio in the CH_3OD system. Both are 0.5 ± 0.1. No large isotope effect is expected in the C−O bond scission processes of the initial insertive complexes, DN−CD_2−OH and HN−CH_2−OD. On the other hand, there must be isotope effects in the H(D) migration processes. In order to produce OD in the CD_3OH system, three D atom migration processes and one H atom migration process are necessary. In the CH_3OD system, one D atom migration process and three H atom migration processes are necessary to produce OH. H atom migration must be more rapid than D atom migration. Nonetheless, the population ratios are the same. This result can be explained by the presence of competitive processes; H(D) atom production processes from the intermediate species. In the CD_3-OH system, the production rate of DN−CHD−OD, the direct precursor of DN═CHD + OD, must be small, but at the same time the decomposition rates of the intermediate species, D_2N−CD−OH and D_2N−CH−OD, to produce DN═C(D)OH + D or DN═C(H)OD + D, must also be small. In methane isotopomer systems, the ejection rate of D is 1/1.3 of that of H.[3] On the other hand, in the CH_3OD system, the production rate of HN−CHD−OH must be large, but the decomposition rates of H_2N−CH−OD and H_2N−CD−OH must also be large. These effects may cancel and the H/D isotope effect in the OH/OD(OD/OH) ratios may disappear. On the other hand, an isotope effect more than that observed in methane isotopomers is expected in the yields of H and D atoms.

NH formation after the insertion of N(^{2}D) into a C−D bond of CD_3OH and H(D) atom migration should be minor, if not completely absent. In order to produce HN−CD_2 −OD from DN−CD_2 −OH, at least six H(D) atom migration processes are necessary. It should be remembered that the rotational and vibrational distributions of NH are highly nonstatistical. The only precursor of NH in the CD_3OH system is CD_3ONH. The situation should be similar in the ND formation process from CH_3OD.

Conclusions

The reactions of N(^{2}D) with CH_3OH and its isotopomers were studied both from experimental and theoretical sides. The most attractive attack site is atomic oxygen. Since atomic oxygen has an unshared electron pair, the additive CH_3O(N)H complex is stable. During the lifetime, an H atom migrates to produce an insertive CH_3ONH complex, which decomposes to CH_3-O + NH or CH_3 + HNO. NH(ND) radicals are also produced when the methyl position is attacked, but this channel is rather minor. OH(OD) radicals are produced after the insertion of N(^{2}D) into a C−H(C−D) bond. Both OH and OD radicals are produced in the reactions with partially deuterated methanols. H(D) atom migration takes place after the insertion. This H(D) atom migration can be related to the triradical character of atomic nitrogen. No H/D isotope effect was observed in the internal energy distributions of NH(ND) and OH(OD), but the rate constants show dependence on the H/D substitution.

Acknowledgment. This work was partially defrayed by the Grant for Basic Science Research Projects of the Sumitomo Foundation. This study was also supported by the REIMEI Research Resources of Japan Atomic Energy Research Institute.

References and Notes

(1) Umemoto, H.; Kimura, Y.; Asai, T. *Chem. Phys. Lett*. **1997**, *264*, 215.
(2) Umemoto, H.; Kimura, Y.; Asai, T. *Bull. Chem. Soc. Jpn.* **1997**, *70*, 2951.
(3) Umemoto, H.; Nakae, T.; Hashimoto, H.; Kongo, K.; Kawasaki, M. *J. Chem. Phys*. **1998**, *109*, 5844.
(4) Umemoto, H.; Asai, T.; Hashimoto, H.; Nakae, T. *J. Phys. Chem. A* **1999**, *103*, 700.
(5) Umemoto, H.; Hachiya, N.; Matsunaga, E.; Suda, A.; Kawasaki, M. *Chem. Phys. Lett*. **1998**, *296*, 203.
(6) Takayanagi, T.; Kurosaki, Y.; Misawa, K.; Sugiura, M.; Kobayashi, Y.; Sato, K.; Tsunashima, S. *J. Phys. Chem. A* **1998**, *102*, 6251.
(7) Takayanagi, T.; Kurosaki, Y.; Sato, K.; Misawa, K.; Kobayashi, Y.; Tsunashima, S. *J. Phys. Chem. A* **1999**, *103*, 250.
(8) Kurosaki, Y.; Takayanagi, T.; Sato, K.; Tsunashima, S. *J. Phys. Chem. A* **1998**, *102*, 254.
(9) Takayanagi, T.; Kurosaki, Y.; Tsunashima, S.; Sato, K. *J. Phys. Chem. A* **1998**, *102*, 10391.
(10) Kurosaki, Y.; Takayanagi, T. *J. Phys. Chem. A* **1999**, *103*, 436.
(11) Alagia, M.; Balucani, N.;Cartechini, L.; Casavecchia, P.; Volpi, G. G.; Sato, K.; Takayanagi, T.; Kurosaki, Y. submitted for publication.
(12) Goldsteijn, N.; Wiesenfeld, J. R. *J. Chem. Phys*. **1983**, *78*, 6725.
(13) Matsumi, Y.; Inagaki, Y.; Kawasaki, M. *J. Phys. Chem*. **1994**, *98*, 3777.
(14) Umemoto, H.; Matsumoto, K. *J. Chem. Phys.* **1996**, *104*, 9640.
(15) Umemoto, H.; Asai, T.; Kimura, Y. *J. Chem. Phys*. **1997**, *106*, 4985.
(16) Umemoto, H. *Chem. Phys. Lett*. **1998**, *292*, 594.
(17) Porter, R. P. *J. Phys. Chem.* **1957**, *61*, 1260.
(18) Brazier, C. R.; Ram, R. S.; Bernath, P. F. *J. Mol. Spectrosc*. **1986**, *120*, 381.
(19) Bogan, D. J.; Setser, D. W. *J. Chem. Phys.* **1976**, *64*, 586.
(20) Matsumi, Y.; Tonokura, K.; Inagaki, Y.; Kawasaki, M. *J. Phys. Chem*. **1993**, *97*, 6816.
(21) Durant, J. L., Jr. *J. Phys. Chem*. **1994**, *98*, 518.
(22) Okada, S.; Tezaki, A.; Miyoshi, A.; Matsui, H. *J. Chem. Phys*. **1994**, *101*, 9582.
(23) Quandt, R. W.; Hershberger, J. F. *J. Phys. Chem*. **1995**, *99*, 16939.
(24) Tsunashima, S.; Morita, K.; Sato, S. *Bull. Chem. Soc. Jpn*. **1977**, *50*, 2283.
(25) Dunning, T. H., Jr. *J. Chem. Phys*. **1989**, *90*, 1007.
(26) Schlegel, H. B. *J. Chem. Phys.* **1986**, *84*, 4530.
(27) Frisch, M. J.; Trucks, G. W.; Schlegel, H. B.; Gill, P. M. W.; Johnson, B. G.; Robb, M. A.;Cheeseman, J. R.; Keith, T.; Petersson, G. A.; Montgomery, J. A.; Raghavachari, K.; Al-Laham, M. A.; Zakrzewski, V. G.; Ortiz, J. V.; Foresman, J. B.; Cioslowski, J.; Stefanov, B. B.; Nanayakkara, A.; Challacombe, M. C.; Peng, Y.; Ayala, P. Y.; Chen, W.; Wong, M. W.; Andres, J. L.; Replogle, E. S.; Gomperts, R.; Martin, R. L.; Fox, D. J.; Binkley, J. S.; Defrees, D. J.; Baker, J.; Stewart, J. P.; Head-Gordon, M.; Gonzalez, C.; Pople, J. A. *Gaussian 94*; Gaussian, Inc.: Pittsburgh, PA, 1995.
(28) Afeefy, H. Y.; Liebman, J. F.; Stein, S. E. *Neutral Thermochemical Data*; Mallard, W. G., Linstrom, P. J., Eds.; 1998.
(29) Schofield, K. *J. Photochem*. **1978**, *9*, 55.